JOURNAL OF MATERIALS SCIENCE 9 (1974) 1689–1695

Ultrafine oxide powders prepared by electron beam evaporation

Part 2 *Powder characteristics*

J. D. F. RAMSAY, R. G. AVERY
Chemistry Division, AERE, Harwell, Oxon, UK

The surface properties and microstructure of ultrafine oxide powders prepared by vapour phase condensation have been examined by several techniques (electron microscopy, X-ray diffraction, nitrogen adsorption isotherms, infra-red absorption of surface species). All the powders had a very small particle size (<20 nm), and gave type II adsorption isotherms – typical of non-porous adsorbents. From infra-red absorption studies of water adsorbed on the surface of the oxides, an unusually relaxed and unreactive surface was indicated.

The compaction and sintering characteristics of the powders were exceptional, and made them highly suited for ceramic fabrication. The contrasting behaviour of an ultrafine magnesia, consisting of porous pseudomorphic agglomerates, is demonstrated.

1. Introduction

Ultrafine powders of several different oxides have been prepared by the vapour phase condensation process already described [1] and some of these have been extensively characterized. In this paper the properties are discussed and compared with those typically observed with ultrafine oxides produced by solid state decomposition reactions. With a view to ceramic applications, special attention is given to the compaction and sintering characteristics of powders, by a comparison of magnesia, formed in the vapour phase, and by thermal decomposition of nesquehonite ($MgCO_3.3H_2O$).

2. Experimental

Adsorption isotherms of N_2 at 77 K on samples of powder were measured volumetrically with an apparatus and in a manner which has been described previously [2]. From the isotherms the specific surface area and pore structure of the samples was determined.

Infra-red spectra of powders, either as deposits on Irtran® discs or as pressed wafers (~0.1 mm thick) were determined using a cell of a type used previously [3]. Samples could thus be outgassed *in situ* at temperatures up to ~ 1200 K.

The densities of sintered oxide compacts were measured by a carbon tetrachloride displacement method. Hot-pressings were made *in vacuo* in a graphite die.

3. Results and discussion

3.1. Physical properties

Typical properties of powders prepared by vapour phase nucleation (in $P_{O_2} > 25$ N m^{-2})

TABLE I Properties of ultrafine oxide powders

	SiO_2	Al_2O_3	ZrO_2	MgO	CaO	CeO_2	U_3O_8
Specific surface area S_{BET}(m^{2}g^{-1})	630	340	250	360	250	170	48
Mean particle size (nm)							
(a) from electron microscopy	4	~5	4	~5	~10	~5	20
(b) from surface area	4.5	6	4.6	4.7	7	8	~25
Crystal phase	amorphous	η-alumina cubic		cubic	cubic	cubic	orthorhombic (a-U_3O_8?)
Bulk density, (kg m^{-3} × 10^3)	0.1	0.05	0.03	0.06	0.1	0.2	0.2

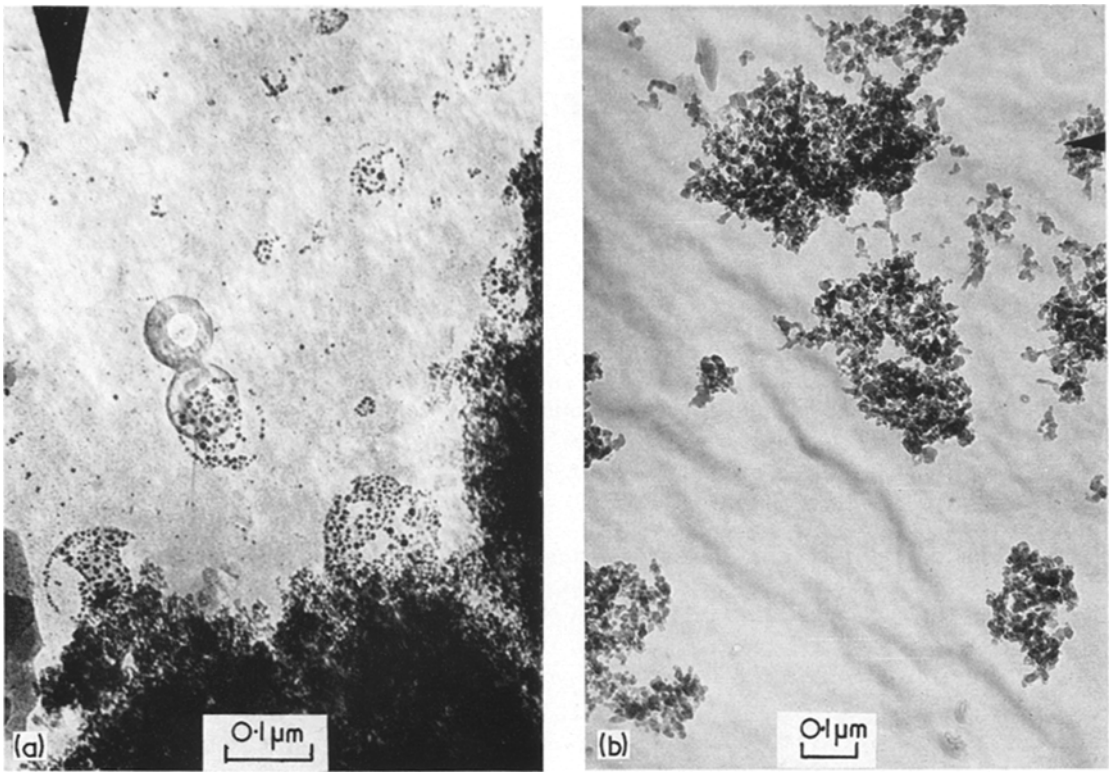

Figure 1 Electron micrographs of oxide powders condensed in the vapour phase, (a) silica, (b) magnesia (run 26), (c) zirconia.

are given in Table I. All the oxides, apart from U_3O_8, had a very high specific surface area (in the range 100 to 800 m^2g^{-1}), and a small particle size with a narrow distribution, as illustrated in the electron micrographs (Fig. 1), and particle size distribution of a silica preparation (Fig. 2). Estimates of particle size from electron microscopy, S_{BET}, and for MgO and ZrO_2, X-ray crystallite size, were in reasonable agreement and indicated that the particles were unaggregated. The relatively low surface area and larger particle size of U_3O_8 may have resulted from an exceptional vapour condensation process, because uraniun dioxide, UO_2, was evaporated (in $P_{O_2} \sim 0.1$ kMn^{-2}), whereas no changes in stoichiometry occurred with the other oxides.

The nitrogen adsorption isotherms of all the powders were of a type II shape in the B.D.D.T. classification [4] (Fig. 5); this is a characteristic feature of non-porous adsorbents, and is unusual with powders of such exceptionally high specific surface area, as has already been described with reference to silica and zirconia [2]. Normalized

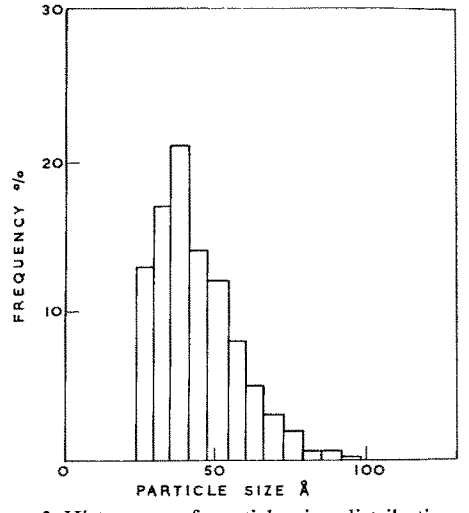

Figure 2 Histogram of particle size distribution of a silica powder preparation.

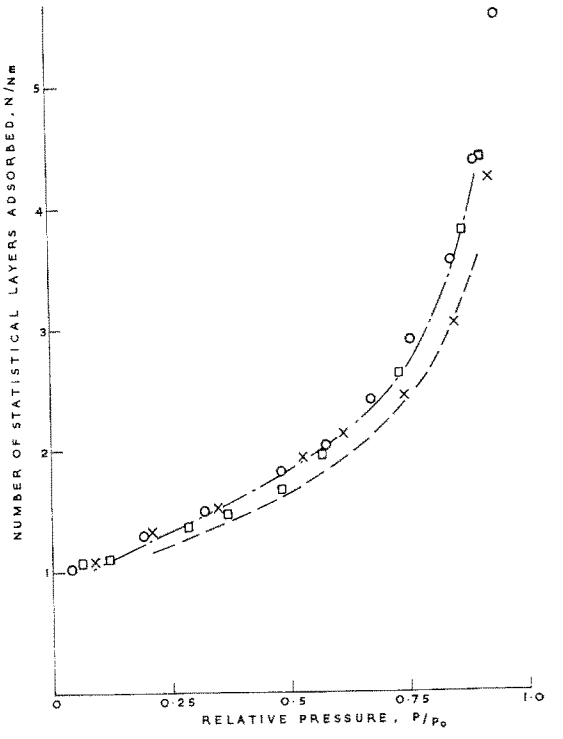

Figure 3 Adsorption isotherms of nitrogen at 77K for: magnesia, ×; alumina, ○; ceria, □, expressed as number of statistical layers adsorbed, N/N_m. The BET monolayer adsorptions N_m (m mol g^{-1}), were: 2.90, 2.76 and 1.75 for MgO, Al_2O_3 and CeO_2, respectively. Standard isotherms for non-porous adsorbents, as reported by Shull [5] and de Boer *et al.* [6] are denoted by curves – – and –·– respectively.

isotherms for magnesia, alumina, and ceria (Fig. 3) were in extremely good accord with the "standard" isotherm for non-porous aluminas and other oxides reported by Shull [5] and de Boer *et al.* [6].

The type II isotherms and very low bulk densities (Table I) of powders produced by vapour condensation indicate a loose assembly of particles in which the number of interparticle contacts is small (2 to 3 per particle). In contrast, ultrafine powders prepared by thermal decomposition of hydrates and salts consist invariably of pseudomorphic agglomerates of particles. These porous agglomerates result in type IV isotherms showing adsorption hysteresis loops [7], which will be exemplified later.

3.2. Bulk and surface purity

The purity of powders was in general > 99.9%, being dependent on that of the evaporated material. Spectrographic analyses of powders derived from mineral periclase and a commercial fused alumina for example were as shown in the table below (major constituents, ppm).

MgO 99.95%						Al_2O_3 99.95%					
Al	30	Ca	50	Mn	10	Ca	50	Mn	10	Ga	50
Na	300	Ni	30	Si	100	Na	100	Si	100		

Anion impurities, which can be considerable in ultrafine oxides produced from decomposition reactions, were exceptionally low.

After preparation and subsequent exposure to air, considerable quantities of water (10 to 20% by weight) were adsorbed by the powders, as would be expected for adsorbents with such a high specific surface area. However, in contrast to oxides of high surface area prepared by thermal decomposition reactions (of hydroxides, carbonates, etc.) the water could be readily desorbed. The steady-state values of water retention after prolonged (~5 to 10 h) pumping of alumina and magnesia at a series of temperatures is shown in Fig. 4. Previous results [8] (curve B) for MgO prepared by dehydration of $Mg(OH)_2$ at 573K correspond to the desorption of strongly physisorbed water up to ~500K; thereafter chemisorbed water, having a statistical

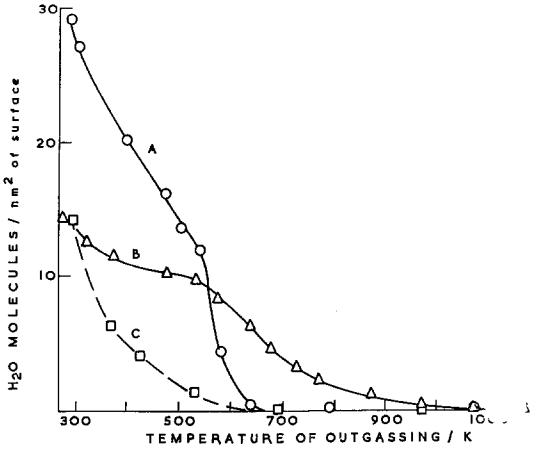

Figure 4 Residual adsorbed water on MgO and Al_2O_3 after prolonged pumping at a series of temperatures; ○, MgO and □, Al_2O_3 prepared by vapour condensation; △, MgO prepared by thermal decomposition of $Mg(OH)_2$ (cf. [8]).

monolayer of ~ 11 mols nm^{-2} is desorbed, requiring a degassing temperature of ~ 1000K for complete removal. With the present magnesia sample (curve A), the final traces of chemisorbed water are removed at ~ 700K. Similar desorption studies made with Al_2O_3, prepared from the hydroxide [9], show that the retention of shemisorbed water corresponds to ~10% of a ctatistical monolayer at 900K in contrast to the result in curve C. A crude estimate of the activation energies for desorption can be derived from the following equation, based on kinetic theory [10]:

$$\sigma \approx 2.6 \times 10^{11} P (MT)^{-\frac{1}{2}} \exp (Q/RT) \text{ mols m}^{-2}$$

where σ is the surface coverage of a gas at a given pressure, P (N m^{-2}), and temperature T(K) having a heat of adsorption, Q. This implies activation energies as high as 200 kJ mol^{-1} for the removal of the last few per cent of water from magnesia and alumina prepared by thermal decomposition, in contrast to ~ 100 kJ mol^{-1} for the corresponding vapour phase preparations.

The high affinity for water can be ascribed to an adsorption at active sites on the surface; these are evidently less numerous on the oxide particles produced by vapour condensation, presumably because crystallization from the liquid phase is sufficiently slow to allow a more stable and uniform arrangement of ions at the surface. Infra-red absorption studies of adsorbed water on ZrO_2, Al_2O_3, SiO_2 and MgO have provided evidence for such a surface configuration [11]. Thus alumina and zirconia powders showed broad adsorption bands in the range 3600 to 3200 cm^{-1} due to physisorbed water, but no evidence of sharp bands in the 3700 to 3800 cm^{-1} region corresponding to chemisorbed –OH groups. The spectrum of silica had a peak of low intensity at 3740 cm^{-1} indicating some chemisorbed –OH groups but was considerably less than observed with Aerosil® and silica gels. The results for magnesia have been reported [11], and again the surface was shown to hydroxylate much less readily than normally observed. These unusual features have been ascribed to an extensive polarization of ions at the oxide surface, in which the cations are displaced inwardly and thence screened by O^{2-} ions. Such a relaxed configuration would have a much reduced specific surface energy, and has been suggested by Weyl [12] to account for the low surface activity of powders calcined above the Tamman temperature.

3.3. Compaction and sintering properties

Exceptionally low porosities ($\epsilon < 0.4$) were obtained on cold compaction ($\geqslant 0{\cdot}5$ GN m^{-2}) of all the ultrafine oxides produced by the present method, as has been described previously for SiO_2 and ZrO_2 powders [13]. This feature can be ascribed to the freedom from agglomeration, and low surface concentration of chemisorbed -OH groups (and in certain cases a uniform spherical particle shape) – characteristics which all aid inter-particle sliding and efficient packing. The marked decrease in pore volume (porosity) of compacts is demonstrated by the N_2 adsorption isotherms (Fig. 5) for ZrO_2; further analysis of the isotherms also shows that all pores within the compacts are extremely small ($\bar{r} < 2$ nm) and have a narrow size distribution [2]. Such a property is highly advantageous in ceramic fabrication since it allows uniform shrinkage of a compact to high density during sintering.

In contrast, ultrafine powders consisting of porous pseudomorphs sinter non-uniformly because of a preferential pseudomorphic shrinkage. This results in a growth, and often isolation, of the larger inter-agglomerate pores; these are subsequently eliminated at higher temperatures, but complete densification is frequently not attained without considerable attendant grain growth [14, 15]. Such contrasting sintering behaviour is illustrated by two different samples of magnesia powder, one (magnesia I) prepared by controlled thermal decomposition of nes-

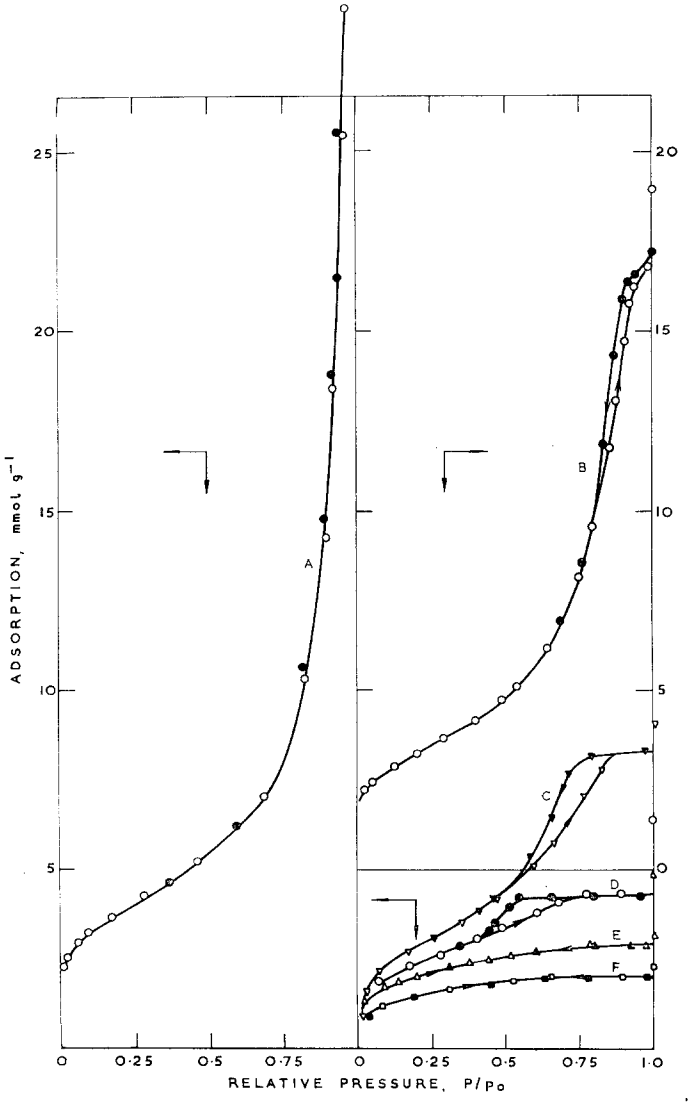

Figure 5 Adsorption isotherms of nitrogen at 77K on zirconia powder and its compacts. A, uncompressed; B, compressed; 46 MN m^{-2}, C, 154 MN m^{-2}; D, 460 MN m^{-2}; E, 1080 MN m^{-2}; F, 1540 MN m^{-2}. Solid symbols denote desorption.

quehonite ($MgCO_3.3H_2O$) *in vacuo* at 698K as described previously [16], the other (magnesia II) by vapour condensation following electron beam evaporation of highly pure periclase. Magnesia I was composed of porous rod-shaped pseudomorphs, whereas magnesia II consisted of discrete unagglomerated particles. The specific surface areas of each sample were very high (319 and 360 m^{2}g^{-1} respectively) and the crystallite size of both $\sim$ 4 nm.

The two types of porosity in magnesia I are demonstrated by the adsorption isotherm (Fig. 6a) which shows two steeply descending sections on the desorption loop – the one at $p/p_0 \sim 0.4$ to 0.5 due to intra-agglomerate pores and the other at $p/p_0 \gtrsim 0.9$ to interagglomerate pores. The pore volume distributions (Fig. 7), corresponding to the isotherms in Fig. 6, and also to compacts of magnesia II (isotherms not shown), illustrate the wide range of pore size caused, before and after compaction, by the interagglomerate pores in magnesia I; the pores (of width $\sim$ 3 nm) in magnesia II have by contrast a narrow size distribution.

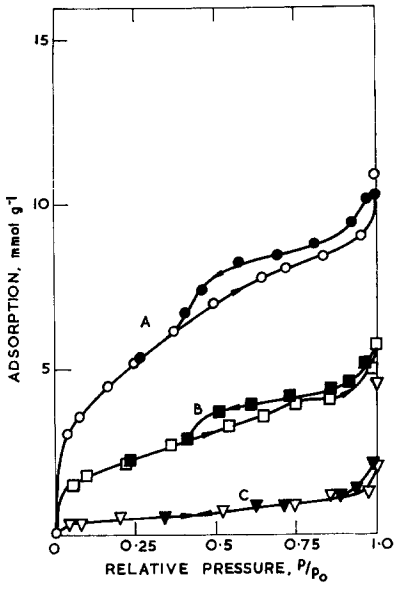

Figure 6 Adsorption isotherms of nitrogen at 77K on magnesia powder [prepared from nesquehonite ($MgCO_3.3H_2O$)], and its compacts. A, uncompressed; compressed: B, 920 MN m^{-2}; C, 1540 MN m^{-2}. Solid symbols denote desorption.

The densification of compacts produced from these two different powders after calcination in air for 8 h at different temperatures is shown in Table II. The densities attained with magnesia I compacts are comparable to those observed by others [17] on firing compacts of ultrafine magnesia at > 1800K, whereas the densities of magnesia II compacts are consistently higher (e.g. $\epsilon \sim 0.07$ and 0.02 respectively at 1773K and 76 MN m^{-2}) under comparable conditions. Such a difference in residual porosity would enhance the physical properties (strength, optical transmittance etc.) of any ceramic fabricated from magnesia II [18].

The hot-pressing characteristics of magnesia II (Fig. 8) are also exceptional and show that rapid sintering begins at temperatures as low as ~ 700K and a relative density of $> 99\%$ is attained at 1273K and a pressure of 82 MN m^{-2}.

Comparable densities, at similar pressures, have only been reported [19] after hot-pressing of ultrafine magnesia powders at temperatures exceeding 1400K.

4. Conclusions

Ultrafine oxide powders with exceptional properties can be produced by vaporisation of bulk oxide with an electron beam and subsequent condensation of vapour species. The properties include very small particle size (<5 nm), large specific surface area (up to $\sim$ 800 m^{2}g^{-1} for SiO_2), non-porous character, low surface and

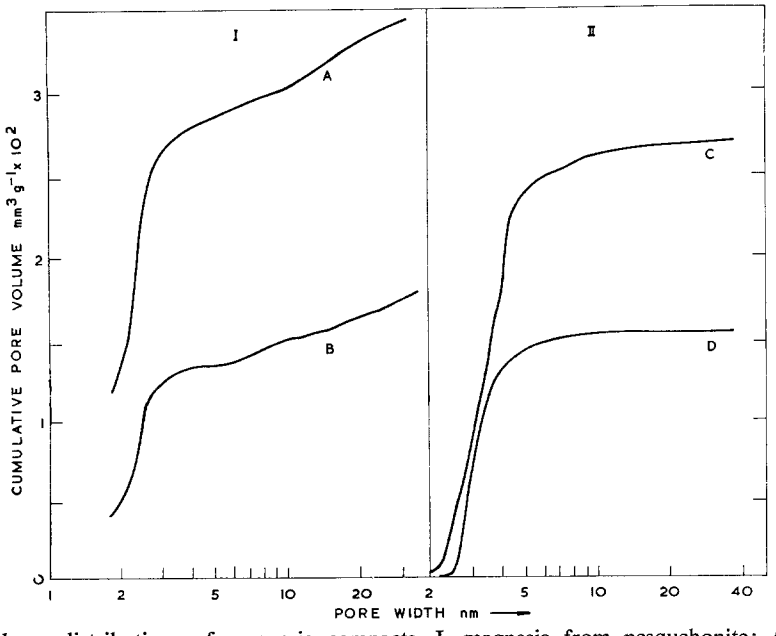

Figure 7 Pore volume distributions of magnesia compacts. I, magnesia from nesquehonite: A, loose powder; compressed, B, 0.92 GN m^{-2}; II, magnesia, unagglomerated: compressed, C, 0.46; D, 0.92 GN m^{-2}.

TABLE II Comparison of the densification of compacts of different magnesia powders; powders were prepared, I from nesquehonite and II by vapour condensation.
Densities (kg $m^{-3} \times 10^3$) are given as a function of precompaction pressure and calcination temperature*

Compaction pressure (GN m^{-2})	Calcination temperature (K)					
	1073		1523		1773	
	I	II	I	II	I	II
0.076	2 99	3.06	3.29	3.38	3.33	3.50
	(0.835)	(0.855)	(0.919)	(0.944)	(0.930)	(0.977)
0.46	3.21	3.31	3.33	3.42	3.36	3.52
	(0.897)	(0.925)	(0.930)	(0.955)	(0.938)	(0.983)
1.54		3.42		3.45		3.55
		(0.955)		(0.964)		(0.992)

*Figures in brackets correspond to relative densities based on an experimental value of 3.58×10^3 kg m^{-3} for periclase crystals.

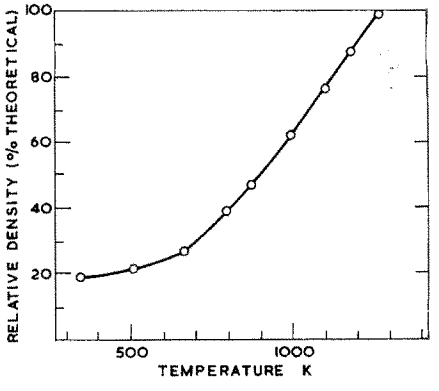

Figure 8 Effect of hot-pressing temperature on the densification of magnesia powder. Samples pressed *in vacuo* at 82 MN m^{-2}; rate of temperature increases was 10K min^{-1}.

bulk contamination; they are somewhat typical of those found with other vapour phase condensation routes, using plasmas. In marked contrast, powders produced by solid-state thermal decomposition reactions, consist invariably of rigid porous pseudomorphs, and are often contaminated with residual anions.

Acknowledgement

The authors are indebted to Mr W. Munro, of Materials Development Division, AERE, for making hot-pressing measurements on magnesia powder.

References

1. J. D. F. RAMSAY and R. G. AVERY, *J. Mater. Sci.* 9 (1974) 1681.
2. R. G. AVERY and J. D. F. RAMSAY, *J. Colloid Interface Sci.* **42** (1973) 597.
3. S. J. GREGG and J. D. F. RAMSAY, *J. Phys. Chem.* **73** (1969) 1243.
4. S. BRAUNAUER, L. S. DEMING, W. S. DEMING and E. J. TELLER, *J. Amer. Chem. Soc.* **62** (1940) 1723.
5. C. G. SHULL, *J. Amer. Chem. Soc.* **70** (1948) 1405.
6. J. H. DE BOER, B. G. LINSEN and T. J. OSINGA, *J. Catalysis* **4** (1965) 643.
7. J. H. DE BOER in "The Strucure and Properties of Porous Materials" edited by D. H. Everett and F. S. Stone (Butterworths, London, 1958) p. 77.
8. P. J. ANDERSON and R. F. HORLOCK, AERE-R4958 (1965).
9. J. B. PERI, *J. Phys. Chem.* **69** (1965) 211.
10. J. H. DE BOER, "The Dynamical Character of Adsorption", (Oxford University Press, 1953).
11. J. D. F. RAMSAY, *Discuss Faraday Soc.* **52** (1972) 49.
12. W. A. WEYL, *J. Colloid Chem.* **6** (1951) 389.
13. J. D. F. RAMSAY and R. G. AVERY, Proceedings of the 1st International Conference on the Compaction and Consolidation of Particulate Matter, Brighton 1972, edited by A. S. Goldberg (Powder Advisory Centre, London, 973) p. 29.
14. I. B. CUTLER, in "High Temperature Oxides", edited by A. M. Alper (Academic Press, London, 1970) Part III, p. 167.
15. J. WILLIAMS, "Science of Ceramics", Vol. 2 (Academic Press, London, 1965) p. 3.
16. P. J. ANDERSON, R. G. AVERY, R. F. HORLOCK and C. W. HUMPHRIES, "Les Solides Finement Divises", edited by J. Ehretsmann (Documentation Française, Paris, 1969) p. 133.
17. D. T. LIVEY, B. M. WANKLYN, M. HEWITT and P. MURRAY, *Trans. Brit. Ceram. Soc.* **56** (1957) 217.
18. See for example, T. VASILOS and W. RHODES in "Ultrafine Grain Ceramics", edited by J. J. Burke, N. L. Reed and V. Weiss (Syracuse University Press, 1970) p. 137.
19. R. W. RICE, *ibid*, p. 203.

Received 9 April and accepted 1 May 1974.